Cannabinoid Receptor Stimulation Impairs Mitochondrial Biogenesis in Mouse White Adipose Tissue, Muscle, and Liver

The Role of eNOS, p38 MAPK, and AMPK Pathways

Laura Tedesco,[1,2] Alessandra Valerio,[1,3] Marta Dossena,[1,3] Annalisa Cardile,[1] Maurizio Ragni,[1] Claudio Pagano,[4] Uberto Pagotto,[5] Michele O. Carruba,[1,2] Roberto Vettor,[4] and Enzo Nisoli[1,2]

OBJECTIVE—Cannabinoid type 1 (CB1) receptor is involved in whole-body and cellular energy metabolism. We asked whether CB1 receptor stimulation was able to decrease mitochondrial biogenesis in different metabolically active tissues of obese high-fat diet (HFD)-fed mice.

RESEARCH DESIGN AND METHODS—The effects of selective CB1 agonist arachidonyl-2-chloroethanolamide (ACEA) and endocannabinoids anandamide and 2-arachidonoylglycerol on endothelial nitric oxide synthase (eNOS) expression were examined, as were mitochondrial DNA amount and mitochondrial biogenesis parameters in cultured mouse and human white adipocytes. These parameters were also investigated in white adipose tissue (WAT), muscle, and liver of mice chronically treated with ACEA. Moreover, p38 mitogen-activated protein kinase (MAPK) phosphorylation was investigated in WAT and isolated mature adipocytes from $eNOS^{-/-}$ and wild-type mice. eNOS, p38 MAPK, adenosine monophosphate–activated protein kinase (AMPK), and mitochondrial biogenesis were investigated in WAT, muscle, and liver of HFD mice chronically treated with ACEA.

RESULTS—ACEA decreased mitochondrial biogenesis and eNOS expression, activated p38 MAPK, and reduced AMPK phosphorylation in white adipocytes. The ACEA effects on mitochondria were antagonized by nitric oxide donors and by p38 MAPK silencing. White adipocytes from $eNOS^{-/-}$ mice displayed higher p38 MAPK phosphorylation than wild-type animals under basal conditions, and ACEA was ineffective in cells lacking eNOS. Moreover, mitochondrial biogenesis was downregulated, while p38 MAPK phosphorylation was increased and AMPK phosphorylation was decreased in WAT, muscle, and liver of ACEA-treated mice on a HFD.

CONCLUSIONS—CB1 receptor stimulation decreases mitochondrial biogenesis in white adipocytes, through eNOS downregulation and p38 MAPK activation, and impairs mitochondrial function in metabolically active tissues of dietary obese mice. ***Diabetes*** **59:2826–2836, 2010**

The expansion of body fat, and particularly of visceral fat, in obese individuals is linked to increased cardiovascular risk. Recent studies have demonstrated that mitochondrial biogenesis and function are decreased in white adipose tissue (WAT), liver, and skeletal muscle of obese/diabetic animals and humans (1). Notably, nitric oxide (NO) generated by endothelial NO synthase (eNOS) increases mitochondrial biogenesis, including peroxisome proliferator–activated receptor γ coactivator-1α (*PGC-1α*) gene expression, in white adipocytes and myocytes (2,3), while genetic eNOS deletion downregulates mitochondrial biogenesis (2,3). Interestingly, eNOS deletion increases p38 mitogen-activated protein kinase (MAPK) activity (4), which can reduce PGC-1α and mitochondrial gene expression (5). On the other hand, the metabolic sensor adenosine monophosphate–activated protein kinase (AMPK) activates eNOS (6), PGC-1α expression, and mitochondrial biogenesis (7).

Cannabinoid type 1 (CB1) receptors control energy metabolism through the modulation of many central and peripheral processes (8). Notably, CB1 receptor–deficient mice are lean (9) and resistant to a high-fat diet (HFD) (10). Similarly, the selective CB1 receptor antagonist SR141716 (rimonabant) persistently reduces body weight of obese mice (11), improving WAT metabolism with reversion of liver steatosis (12) and increasing glucose uptake in skeletal muscle (13). We have recently demonstrated that both genetic and pharmacological blockade of CB1 receptor increases AMPK activity, mitochondrial biogenesis and function in WAT of HFD-fed mice, in an eNOS-dependent manner, to the levels of chow regular diet-fed controls (14). This is accompanied by a reduced body weight gain and adiposity.

Since the endocannabinoid system is overactive in peripheral organs, and particularly in the visceral fat of obese subjects, while circulating levels of endocannabinoids are elevated in type 2 diabetic patients (15), our previous results suggested that the CB1 receptor overstimulation, by downregulating mitochondrial biogenesis in metabolically active tissues, could partly justify the increased fat depots and metabolic dysfunctions in obese

From the [1]Integrated Laboratories Network, Center for Study and Research on Obesity, and the Department of Pharmacology, Chemotherapy and Medical Toxicology, School of Medicine, University of Milan, Milan, Italy; [2]Istituto Auxologico Italiano, Milan, Italy; the [3]Department of Biomedical Sciences and Biotechnologies, University of Brescia, Brescia, Italy; the [4]Endocrine-Metabolic Laboratory, Internal Medicine, Department of Medical and Surgical Sciences, University of Padova, Padova, Italy; and the [5]Endocrinology Unit, Department of Internal Medicine and Gastroenterology, and the Center for Applied Biomedical Research S. Orsola-Malpighi Hospital, Alma Mater Bologna University, Bologna, Italy.

Corresponding author: Enzo Nisoli, enzo.nisoli@unimi.it.

Received 23 December 2009 and accepted 6 August 2010. Published ahead of print at http://diabetes.diabetesjournals.org on 25 August 2010. DOI: 10.2337/db09-1881.

L.T. and A.V. contributed equally to this work.

rodents. The present study analyzed the in vitro and in vivo effects of endocannabinoid receptor agonists, including 2-arachidonoyl-glycerol (2-AG) and anandamide (AEA), and selective CB1 agonist, such as arachidonyl-2-chloroethanolamide (ACEA) (16), on mitochondrial biogenesis in primary white adipocytes and WAT, liver, and skeletal muscle of lean and obese mice. Moreover, the role of eNOS, p38 MAPK, and AMPK pathways in this process was investigated.

RESEARCH DESIGN AND METHODS

Cell culture and reagents. White fat precursor cells were enzymatically isolated from epididymal WAT of 8-week-old male C57BL/6J, wild-type (F2 hybrid B6.129S2 obtained from crossing C57BL/6J and 129S1/SvImJ mice), and B6.129P2-Nos3^{tm1Unc}/J (eNOS$^{-/-}$) mice (17) (The Jackson Laboratories, Bar Harbor, ME) and cultured as previously described (14). At day 3–4 from seeding, cells were exposed to the culture medium containing CB1 agonists for 48 h or different periods of time when specified. The medium was discarded, the wells were washed twice with 2 ml ice-cold phosphate-buffered solution (PBS) (Sigma-Aldrich), and the cells were harvested as reported below for the different assays. Primary human subcutaneous and visceral preadipocytes, isolated from subcutaneous and visceral/abdominal tissue (kidney and bladder) of normal weight subjects without metabolic disorders, together with specific growth media, were purchased from Lonza (Walkersville, MD). SB203580 and SB202190 were obtained from Tocris Bioscience (Bristol, U.K.). All other chemicals, including ACEA, 2AG, and AEA, were purchased from Sigma (Milan, Italy).

CB1 siRNA and p38MAPK siRNA. White adipocytes were transfected at day 3–4 after seeding with 10 nmol/l CB1 or 50 nmol/l p38MAPK siRNA SMARTpool (Dharmacon, Lafayette, CO) or *siCONTROL* nontargeting siRNA using Dharmafect three transfection reagent. Cells were treated for 48 h with 0.01 μmol/l ACEA, and RNA and protein were harvested. Efficacy of transfection was determined using si*GLO*-RISC-free nontargeting siRNA and estimation of siRNA uptake by fluorescence detection (absorbance/emission 557/570 nm).

Animals and treatments. The animals were treated according to protocols approved by the Milan University Institutional Animal Care and Use Committee. In particular, 8-week-old (n = 20) male wild-type and eNOS$^{-/-}$ mice (17) were housed four per cage. Moreover, 4-week-old male C57BL/6J mice (Harlan Nossan) were fed either a chow regular diet (Chow) (8 kcal % fat, 19 kcal % protein, 73 kcal % carbohydrate) or a high-fat diet (HFD) (45 kcal % fat, 20 kcal % protein, and 35 kcal % carbohydrate, D12451; Research Diets, New Brunswick, NJ) for 6 weeks before treatments. While fed on chow or a HFD, these mice (n = 10 per group) were further treated with either vehicle or ACEA (at 2.5 mg/kg i.p.) for 4 weeks. To avoid potential habituation, ACEA doses were increased through time as treatment advanced as follows: 1.25 mg/kg on days 1–3, 1.9 mg/kg on days 4–6, and 2.5 mg/kg for the rest of treatment (18). Mice did not display signs of catalepsy (as frozen postures or immobility) (data not shown). Body weight and food intake were recorded weekly. Adiposity (wet weight of visceral and subcutaneous fat), cumulative food intake (for the time of the experiment), and feed efficiency were measured (2). On the day of the experiments, animals were killed by cervical dislocation and epididymal WAT was immediately isolated, frozen in liquid nitrogen, and stored at −80°C before processing for mRNA, protein, and citrate synthase analysis.

Isolation of mouse mature adipocytes. Wild-type and eNOS$^{-/-}$ mice, both on the chow regular diet (n = 6 per group), were killed, and epididymal WAT was excised. Fat pads from two mice were pooled, and mature adipocytes were acutely isolated in Hank's balanced salt solution (HBSS) containing 4% bovine serum albumin (BSA) and 1.5 mg/ml collagenase (Calbiochem) as previously described (19).

RNA analysis. Quantitative RT-PCR reactions were performed as previously described (14) and run with the iQ SybrGreenI SuperMix (Bio-Rad) on an iCycler iQ Real Time PCR detection system (Bio-Rad). Calculations were performed by a comparative method ($2^{-\Delta\Delta Ct}$) using 18S rRNA as an internal control. Primers were designed using Beacon Designer 2.6 software (Premier Biosoft International).

Immunoblot analysis. Protein extracts were analyzed by immunoblotting as previously described (14). Protein extracts were obtained by harvesting cultured adipocytes in M-PER Mammalian Protein Extraction Reagent as indicated by the manufacturer in the presence of 1 mmol/l $NaVO_4$, 10 mmol/l NaF, and a cocktail of protease inhibitors (Sigma-Aldrich). Protein content was determined by the bicinchoninic acid protein assay (Pierce), and 50 μg proteins were run on SDS-PAGE under reducing conditions. The separated proteins were then electrophoretically transferred to a nitrocellulose membrane (Pierce). Proteins of interest were revealed with specific antibodies: anti-eNOS (Transduction Labs), anti–cytochrome c oxidase IV (COX IV) (Molecular Probes), and anti–cytochrome c (Cyt c) (BD Bioscience), each at 1:500 dilution; anti–phospho–p38 MAPK (Thr180/Tyr182) and anti–p38 MAPK (both at 1:1,000 dilution; Cell Signaling Technology); anti–phospho–AMPKα (Thr172) and anti–AMPKα (both at 1:1,000 dilution; Cell Signaling Technology); and anti–β-actin (1:10,000; Sigma-Aldrich). The immunostaining was detected using horseradish peroxidase–conjugated anti-rabbit or anti-mouse immunoglobulin for 1 h at room temperature. After the visualization of phospho–p38 MAPK or phospho-AMPKα, filters were stripped with the Re-Blot Western blot recycling kit (Chemicon International) and further used for the visualization of total p38 MAPK or AMPKα. Bands were revealed by the SuperSignal Substrate (Pierce) and quantitated by densitometry using a Quick Image densitometer (Canberra Packard) and a Phoretix 1D, version 3.0, software image analyser.

Mitochondrial DNA. Mitochondrial DNA copy number was measured by means of quantitative PCR from the cytochrome C oxidase II mtDNA gene compared with the *UCP2* nuclear gene in tissues of ACEA-treated mice and wild-type mice fed either chow or a HFD as previously described (14).

Oxygen consumption. White adipocytes were harvested by trypsinization, centrifuged at 500*g* for 5 min at 4°C, and resuspended in HBSS. Cell samples (4×10^6/ml) were analyzed at 37°C in a gas-tight vessel equipped with a Clark-type oxygen electrode (Rank Brothers) connected to a chart recorder. Cellular oxygen consumption was measured as previously described (14). The oxygen electrode was calibrated, assuming the concentration of oxygen in the incubation medium at 37°C to be 200 μmol/l. Protein content in both cell and tissue samples was determined by the bicinchoninic acid protein assay (Pierce).

Mitochondrial mass. White adipocytes seeded onto glass coverslips were incubated with medium containing 200 nmol/l Mitotracker red 580 (Invitrogen). After incubation for 30 min at 37°C, coverslips were rinsed two times with medium and two times with PBS and fixed at room temperature for 10 min in 4% paraformaldehyde in PBS. Coverslips were mounted onto glass slides and were then observed with a Bio-Rad confocal microscope MRC1024.

Citrate synthase activity and statistical methods. The activity was measured spectrophotometrically at 412 nm at 30°C in either tisssue or whole cell extracts (14). Tissue or cell homogenates were added to buffer containing 0.1 mmol/l 5,5-dithio-bis-(2-nitrobenzoic) acid, 0.5 mmol/l oxaloacetate, 50 μmol/l EDTA, 0.31 mmol/l acetyl CoA, 5 mmol/l triethanolamine hydrochloride, and 0.1 mol/l Tris-HCl, pH 8.1. Citrate synthase activity was expressed as nanomoles citrate produced per minute per milligram of protein or relative values. Raw data from each experiment were analyzed using either ANOVA with Newman-Keuls' multiple comparison post hoc test or t test.

RESULTS

ACEA decreases mitochondrial biogenesis in mouse white adipocytes. CB1 receptor stimulation by ACEA, AEA, and 2-AG downregulated mitochondrial biogenesis in a reversed concentration-dependent manner in cultured mouse white adipocytes (Fig. 1 and supplementary Fig. 1, available in the online appendix [http://diabetes.diabetesjournals.org/cgi/content/full/db09-1881/DC1]). In particular, the effects of ACEA, tested on several mitochondrial markers, were most evident at 0.01 μmol/l, with higher concentrations being less effective (Fig. 1) and lower concentrations (0.01–1.0 nmol/l) lacking efficacy (supplementary Fig. 2). The mRNA levels of PGC-1α, nuclear respiratory factor-1 (NRF-1), and mitochondrial DNA transcription factor A (Tfam) (three key regulators of mitochondrial biogenesis) (20), as well as the mtDNA amount, were lower in ACEA- than in vehicle-treated cells (Fig. 1*A* and *B*). Protein levels of COX IV and Cyt c (two mitochondrial proteins involved in oxidative phosphorylation) (Fig. 1*C*), activity of citrate synthase (Fig. 1*D*), and oxygen consumption (Fig. 1*E*) were decreased by the CB1 receptor stimulation. Furthemore, white adipocytes treated with ACEA showed a significant decrease of MitoTracker Red signal, indicating the decrease of mitochondrial mass compared with vehicle-treated cells (Fig. 1*F*). Similar results were obtained with AEA and 2-AG (supplementary Fig. 1).

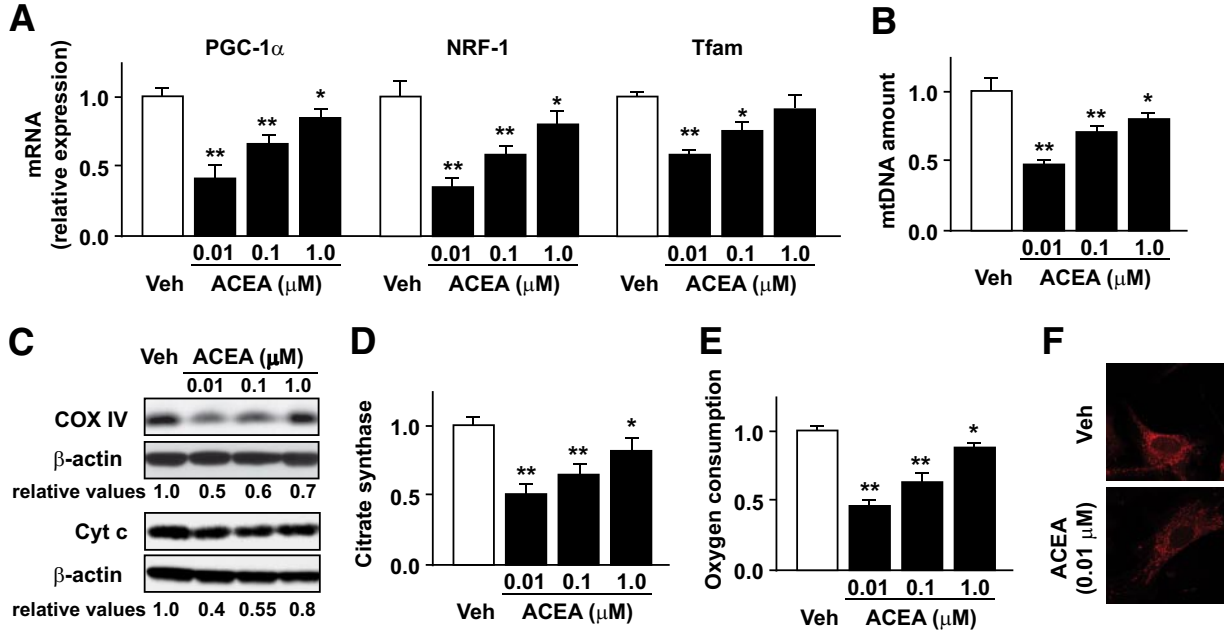

FIG. 1. The CB1 receptor agonist ACEA decreases mitochondrial biogenesis in cultured mouse white adipocytes. *A*: PGC-1α, NRF-1, and Tfam mRNA levels were analyzed by means of quantitative RT-PCR in white adipocytes treated either with vehicle (0.002% DMSO) (Veh) or different doses of ACEA for 2 days. Relative expression values of the vehicle-treated cells were taken as 1.0 ($n = 5$ experiments; *$P < 0.05$ and **$P < 0.01$ vs. vehicle-treated cells). *B*: mtDNA amount, analyzed by means of quantitative PCR and expressed as mtDNA copy number per nuclear DNA copy number. *$P < 0.05$ and **$P < 0.01$ vs. vehicle-treated cells. *C*: COX IV and Cyt c proteins were detected by immunoblot analysis (one experiment representative of five reproducible ones). Numbers below the blots are values of densitometric analysis referring to β-actin. *D* and *E*: Citrate synthase activity (nmol citrate · min^{-1} · mg^{-1} protein) (*D*) oxygen consumption (nmol O_2 · min^{-1} · mg^{-1} protein) (*E*) were expressed as fold change vs. vehicle-treated cells taken as 1.0 ($n = 3$ experiments; *$P < 0.05$ and **$P < 0.01$ vs. vehicle-treated cells). All data represent means ± SEM. *F*: Mitochondrial mass in white fat cells visualized as MitoTracker Red signal by confocal microscopy. Images were acquired by using a ×40 objective. (A high-quality color representation of this figure is available in the online issue.)

ACEA decreases mitochondrial biogenesis in human subcutaneous and visceral white adipocytes. CB1 receptor stimulation by ACEA downregulated mitochondrial biogenesis in cultured subcutaneous and visceral white adipocytes of normal-weight subjects. A significant reduction of PGC-1α, NRF-1, and Tfam mRNA levels was observed in subcutaneous and visceral white adipocytes exposed for 2 days to 0.01 μmol/l ACEA (supplementary Fig. 3*A*). Similarly, the mtDNA amount, COX IV and Cyt c protein levels, citrate synthase activity, and oxygen consumption were decreased by the CB1 receptor stimulation (supplementary Fig. 3*B*–*E*). All of these effects were dose dependent, with maximal effect at 0.01 μmol/l ACEA (data not shown). Although the expression of CB1 receptor was reported to be higher in the subcutaneous than in the visceral fat of lean subjects (21), no relevant difference in the ACEA effects on mitochondrial biogenesis were seen between human subcutaneous and visceral adipocytes. Further analysis will be necessary to clarify this point.

NO-generating pathway is involved in ACEA effects on mitochondrial biogenesis. Given that eNOS stimulation was reported to increase mitochondrial biogenesis in WAT cells (2) and that CB1 receptor blockade promotes mitochondrial biogenesis by upregulating eNOS (14), we hypothesized that the inhibitory effects of CB1 agonists on mitochondrial biogenesis could be due to downregulation of eNOS expression and NO production. ACEA significantly decreased eNOS mRNA (Fig. 2*A*) and protein levels (Fig. 2*B*) in primary mouse white adipocytes. To verify that the downregulation of eNOS by ACEA is a relevant molecular mechanism by which mitochondrial biogenesis is affected, mouse fat cells were treated with 0.01 μmol/l ACEA in the presence of two structurally unrelated NO donors. (Z)-1-[2-(2-aminoethyl)-N-(2-ammonioethyl)amino]-diazen-1-ium-1,2-diolate] (DETA-NO) (50 μmol/l) prevented the effect of ACEA on mitochondrial biogenesis with a full restoration of PGC-1α, NRF-1, Tfam, COX IV, and Cyt c expression and mtDNA amount in fat cells (Fig. 2*C* and *D*). Similar results were obtained with 100 μmol/l S-nitroso-acetyl penicillamine (SNAP) (data not shown).

ACEA affects mitochondrial biogenesis through CB1 receptor stimulation. Prolonged exposure of white adipocytes to different concentrations of ACEA did not modify CB1 receptor mRNA levels (supplementary Fig. 4*A*). CB2 mRNA levels were decreased by ACEA treatment (supplementary Fig. 4*B*). Because CB1 agonists induce adipocyte differentiation (15,22), the latter result may reflect the reduction of CB2 receptors that accompanies adipocyte differentiation (22). To assess the CB1 receptor dependence of ACEA effects on eNOS expression and mitochondrial biogenesis, primary white adipocytes were transfected with small interference RNA (siRNA) against CB1 receptor or nontargeting siRNA as a negative control. We verified that CB1 siRNA reduced CB1 receptor mRNA levels by 85% (Fig. 3*A*). While white adipocytes treated with 0.01 μmol/l ACEA showed decreased eNOS mRNA, CB1 receptor knockdown reduced the inhibitory effects of ACEA with a partial, albeit statistically significant, recovery of eNOS expression (Fig. 3*B*). Accordingly, a partial recovery of mitochondrial gene expression, mtDNA amount, and citrate synthase activity was observed (Fig. 3*C*–*E*). Importantly, the CB1 silencing per se did not modify any mitochondrial biogenesis parameters. Thus, our present results suggest that the effects of ACEA on eNOS expression and mitochondrial biogenesis are at least in part mediated by the CB1 receptors in white adipocytes.

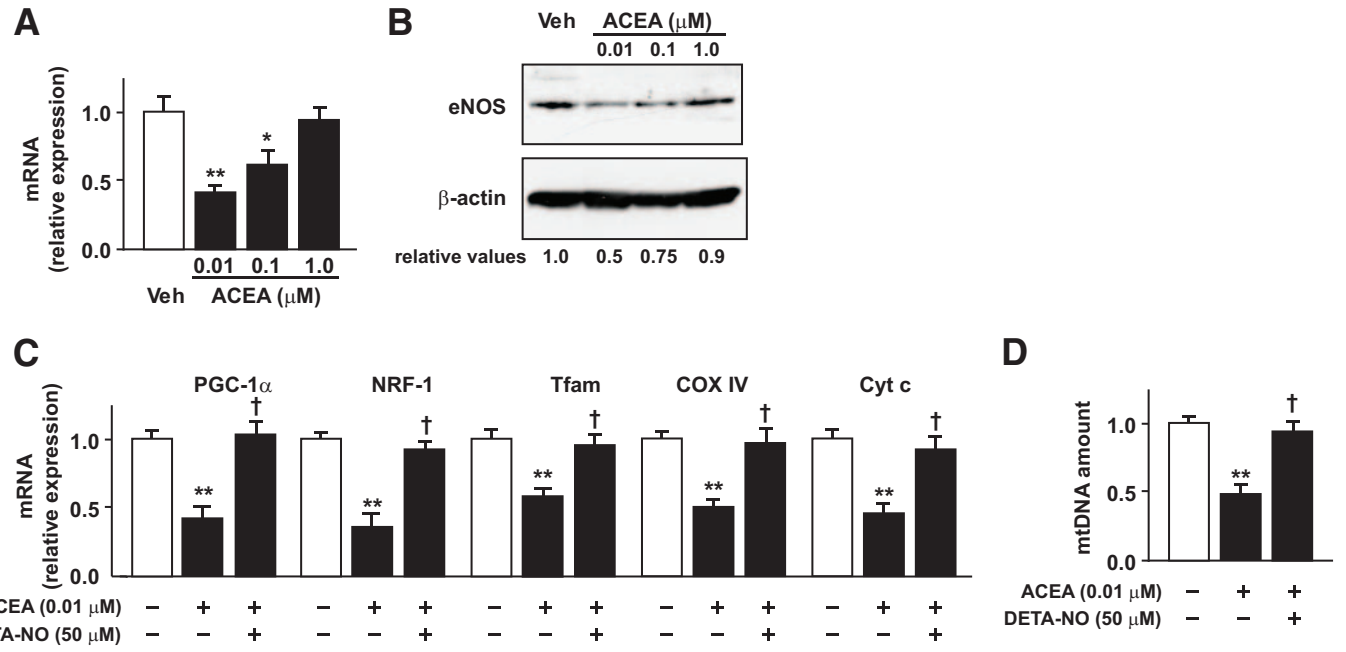

FIG. 2. ACEA downregulates eNOS expression in cultured mouse white adipocytes. *A* and *B*: eNOS mRNA and protein, analyzed by quantitative RT-PCR and immunoblotting, in vehicle-treated cells (0.002% DMSO) (Veh) or after exposure to different doses of ACEA for 2 days. *A*: Relative expression values of the vehicle-treated cells were taken as 1.0 (n = 5 experiments; *P < 0.05 and **P < 0.01 vs. vehicle). *B*: One experiment representative of five reproducible ones. Numbers below the blots are values of densitometric analysis referring to β-actin. *C*: PGC-1α, NRF-1, Tfam, COX IV, and Cyt c mRNA in white adipocytes treated with ACEA alone or in combination with DETA-NO for 2 days. Relative expression values of the untreated cells were taken as 1.0 (n = 4 experiments; **P < 0.01 vs. vehicle-treated cells and †P < 0.05 vs. ACEA-treated cells). *D*: mtDNA amount, expressed as mtDNA copy number per nuclear DNA copy number. **P < 0.01 vs. vehicle-treated cells. †P < 0.05 vs. ACEA-treated cells. All data represent means ± SEM.

However, we investigated the potential involvement of another reported target of low concentrations (in micromoles) of ACEA, i.e., the transient receptor potential vanilloid subfamily type 1 (TRPV1) (23). This receptor is expressed in preadipocytes and at a lower amount also in adipocytes (24), where its activation reduces lipogenesis, possibly exerting effects opposite to those of CB1 stimulation (24). Primary white adipocytes were transfected with siRNA against TRPV1 receptor or nontargeting siRNA as a negative control. We verified that TRPV1 siRNA reduced TRPV1 receptor mRNA levels by 80% (supplementary Fig. 5). Notably, TRPV1 receptor knockdown left unchanged the inhibitory effects of 0.01 μmol/l ACEA on eNOS and mitochondrial gene expression, mtDNA amount, and citrate synthase activity (supplementary Fig. 5).

ACEA induces p38 MAPK activation via eNOS downregulation. Increasing evidence suggests that a link exists between NO/eNOS and p38 MAPK activity in various cell types (4,25). In particular, p38 MAPK phosphorylation is increased in ventricular cardiomyocytes of eNOS knockout mice (4). Actually, we found that p38 MAPK phosphorylation was 90 ± 4% higher in WAT of eNOS$^{-/-}$ compared with littermate control mice (Fig. 4*A*).

Because WAT contains different cell types besides adipocytes, mature white adipocytes were acutely isolated from epididymal fat pad of eNOS$^{-/-}$ and wild-type littermates on the chow regular diet. Again, isolated adipocytes with eNOS gene deletion showed strongly increased p38 MAPK phosphorylation (Fig. 4*B*). CB1 receptor stimulation can activate p38 MAPK (26). Treatment of cultured white adipocytes with 0.01 μmol/l ACEA increased p38 MAPK phosphorylation within 30 min, and this effect persisted until 24 h (representative data are shown at 1 h [Fig. 4*C*]). Further, primary white adipocytes from eNOS$^{-/-}$ mice showed increased phospho–p38 MAPK protein compared with primary adipocytes from wild-type mice (Fig. 4*D*). Interestingly, ACEA (0.01 μmol/l for 1–16 h) was unable to increase p38 MAPK phosphorylation in primary white adipocytes obtained from eNOS$^{-/-}$ knockout unlike that from wild-type mice (Fig. 4*D*), suggesting that p38 MAPK activation by ACEA occurs via eNOS downregulation. Accordingly, ACEA was ineffective at further decreasing the impaired mitochondrial biogenesis in white adipocytes lacking eNOS (data not shown).

ACEA affects mitochondrial biogenesis through p38 MAPK activation. Because p38 MAPK activation has been reported to decrease PGC-1α expression in C2C12 cells (5), we investigated whether p38 MAPK was involved in mitochondrial biogenesis downregulation by ACEA. Treatment with p38 MAPK inhibitors SB203580 and SB202190 prevented the 0.01 μmol/l ACEA-induced decreases in PGC-1α, NRF-1, and Tfam mRNA levels (Fig. 5*A*), mtDNA amount (Fig. 5*B*), and citrate synthase activity (Fig. 5*C*).

Because pharmacological inhibitors are often nonspecific, white adipocytes were transfected with siRNA directed against p38α MAPK or nontargeting siRNA as a negative control. The p38 MAPK mRNA levels were reduced by 75 ± 3% (Fig. 5*D*), while the p38 MAPK protein levels were reduced by 60 ± 3% (Fig. 5*E*) in p38α MAPK siRNA-treated cells. Importantly, the p38α MAPK silencing prevented the 0.01 μmol/l ACEA-mediated downregulation of PGC-1α, NRF1, and Tfam (Fig. 5*F*) and the reduction of mtDNA amount (Fig. 5*G*), confirming a mechanistic role for the p38 MAPK-dependent pathways in mediating the effects of ACEA on mitochondrial biogenesis in fat cells.

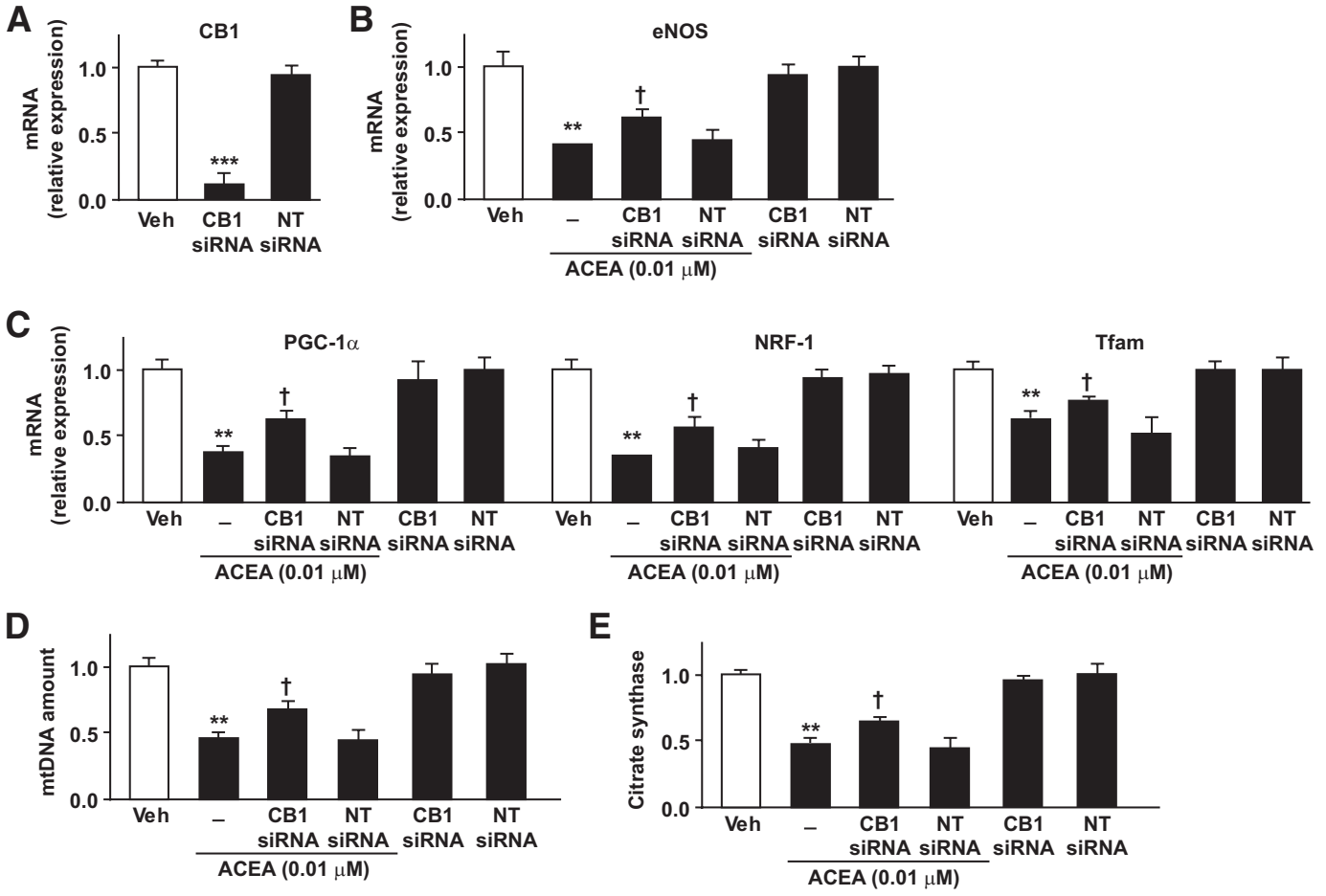

FIG. 3. ACEA decreases mitochondrial biogenesis through CB1 receptor stimulation in cultured mouse white adipocytes. *A*: CB1 receptor expression in white adipocytes transfected with either CB1 siRNA or nontargeting siRNA. ***$P < 0.001$ vs. vehicle-treated cells. *B–E*: mitochondrial biogenesis parameters in white adipocytes transfected with either CB1 siRNA or nontargeting siRNA and treated with vehicle (0.002% DMSO) (Veh) or with ACEA for 2 days. *B*: eNOS expression. *C*: PGC-1α, NRF-1, and Tfam expression. Relative expression values of the vehicle-treated cells were taken as 1.0 ($n = 5$ experiments; **$P < 0.01$ vs. vehicle-treated cells and †$P < 0.05$ vs. ACEA-treated cells). *D*: mtDNA amount. *E*: Citrate synthase activity. **$P < 0.01$ vs. vehicle-treated cells. †$P < 0.05$ vs. ACEA-treated cells. All data represent means ± SEM.

ACEA inhibits AMPK phosphorylation. We demonstrated that CB1 receptor blockade increased AMPK phosphorylation and activity in cultured white adipocytes (14). Since the AMPK cascade has been described to activate eNOS and NO production (6), we hypothesized that AMPK might be involved in the effect of CB1 receptor stimulation on mitochondrial biogenesis. In fact, treatment of cultured white adipocytes with 0.01 μmol/l ACEA reduced AMPK phosphorylation (supplementary Fig. 6).

CB1 receptor agonist downregulates mitochondrial biogenesis in metabolically active tissues and increases body weight in obese mice. To assess whether the cannabinoid receptor stimulation decreases mitochondrial biogenesis in vivo, we examined the eNOS expression and markers of mitochondrial biogenesis in epididymal fat pads, tibialis muscle, and liver derived from male mice on either the chow regular diet or HFD for 6 weeks and then treated with ACEA (2.5 $mg \cdot kg^{-1} \cdot day^{-1}$ i.p.) (16,18) or vehicle for 4 weeks. No effect was seen in chow regular diet–fed mice (Fig. 6 and supplementary Figs. 7 and 8). As expected (27), HFD reduced eNOS expression and mitochondrial biogenesis in WAT of untreated mice (Fig. 6). This effect was observed also in muscle and liver (supplementary Figs. 7 and 8). Although eNOS expression was unchanged in WAT (Fig. 6*A*), it was decreased in muscle and liver (supplementary Figs. 7*A* and 8*A*), and the mRNA levels of PGC-1α, NRF-1, and Tfam and the mtDNA amount were lower in WAT (Fig. 6*B* and *C*), muscle (supplementary Fig. 7*B* and *C*), and liver (supplementary Fig. 8*B* and *C*) of ACEA-treated HFD mice than in those of vehicle-treated HFD mice. Also, COX IV and Cyt c protein levels and citrate synthase activity were lower in WAT (Fig. 6*D* and *E*), muscle (supplementary Fig. 7*D* and *E*), and liver (supplementary Fig. 8*D* and *E*) of ACEA-treated HFD mice than in those of vehicle-treated HFD mice. Further, ACEA treatment increased p38 MAPK phosphorylation in WAT, muscle, and liver of HFD mice (Fig. 6*F* and supplementary Figs. 7*F* and 8*F*). We previously found that AMPK activity was reduced in WAT of HFD-fed mice (14). Noticeably, ACEA treatment decreased AMPK phosphorylation in WAT (Fig. 6*G*), muscle (supplementary Fig. 7*G*), and liver (supplementary Fig. 8*G*) of HFD mice.

Interestingly, unlike chow regular diet–fed mice, the mean body weight and adiposity of the ACEA-treated mice were higher compared with those of the vehicle-treated mice on the HFD (Fig. 7*A* and *B*). Cumulative food intake was comparable between the two groups (Fig. 7*C*), although ACEA-treated mice showed a greater feed efficiency than their vehicle-treated controls (Fig. 7*D*). These results suggest that a CB1 receptor stimulation may impair the oxidative metabolism in WAT, muscle, and liver and

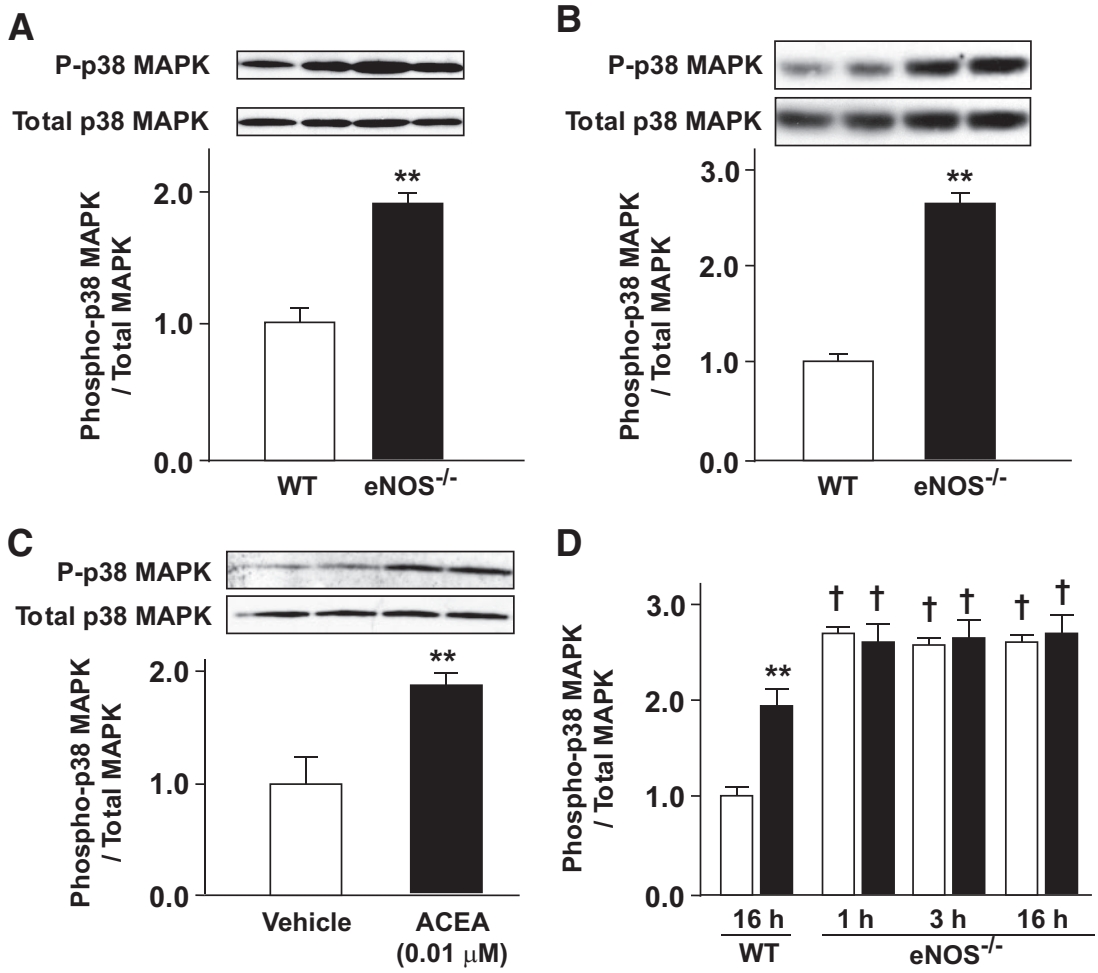

FIG. 4. Phosphorylation of p38 MAPK depends on eNOS in WAT and white adipocytes. *A*: p38 MAPK phosphorylation in WAT obtained from WT and eNOS$^{-/-}$ mice. *B*: p38 MAPK phosphorylation in mature white adipocytes isolated from wild-type and eNOS$^{-/-}$ mice. *A* and *B*: Representative immunoblots of five reproducible ones. Bar graphs show the densitometric quantification of the blots (phospho–p38 MAPK normalized to total p38 MAPK) with wild-type values taken as 1.0. **$P < 0.01$ vs. wild-type. *C*: p38 MAPK phosphorylation in primary white adipocytes treated for 1 h with vehicle (0.002% DMSO) (Veh) or ACEA. Values from the densitometric analysis are shown with vehicle values taken as 1.0. **$P < 0.01$ vs. vehicle. *D*: p38 MAPK phosphorylation in primary white adipocytes from WT and eNOS$^{-/-}$ mice exposed to vehicle (open bars) or to 0.01 μmol/l ACEA (closed bars). Values from the densitometric analysis are shown with untreated wild-type values taken as 1.0. **$P < 0.01$ vs. untreated wild-type adipocytes. †$P < 0.05$ vs. ACEA-treated WT adipocytes. All data represent means ± SEM.

lead to further increase of body weight and adiposity in obese animals on a HFD.

DISCUSSION

We have previously demonstrated that both genetic (CB1 knockout mice) and pharmacological (SR141716-treated mice) blockade of the cannabinoid CB1 receptor increases mitochondrial biogenesis in an eNOS-dependent manner and enhances AMPK activity in white adipocytes and WAT (14), possibly antagonizing an endocannabinoid tone present in cultured fat cells and in fat. The present study clearly demonstrates that ACEA and endocannabinoid receptor agonists downregulate mitochondrial biogenesis and function in mouse and human primary white adipocytes. In particular, the expression of PGC-1α, which coordinately regulates the entire mitochondrial biogenesis program (20), was markedly and concentration-dependently decreased by the cannabinoid agonists. Mitochondrial mass and function were decreased as well.

Notably, the CB1 receptor stimulation decreases mitochondrial biogenesis in metabolically active tissues, including WAT, muscle, and liver, in vivo. Four week treatment with ACEA, at a concentration that does not impair locomotor activity or induce evident side effects (18), reduced mitochondrial biogenesis in obese mice (i.e., HFD-fed mice). Although food intake was comparable between the two groups, feed efficiency was higher in the ACEA-treated than in the vehicle-treated obese mice, suggesting that the whole-body oxidative metabolism is decreased in the drug-treated animals. Accordingly, the body weight and adiposity of treated obese mice were higher compared with those of the vehicle-treated obese animals. On the contrary, ACEA was ineffective in chow regular diet–fed mice. In line with previous reports (28), food intake measured 1–3 h after the first ACEA administration was transiently increased in both lean and HFD mice (data not shown). A few hypotheses may be offered to explain the lack of ACEA effects in lean mice after chronic treatment. Since cannabinoid/CB1 signaling is overactive in the peripheral tissues of HFD mice, including WAT (15,22), it is possible that ACEA only worked in these mice as a result of additive effects with the enhanced endogenous tone. Furthermore, like AEA, ACEA is degraded by the enzyme fatty acid amide hydrolase (FAAH),

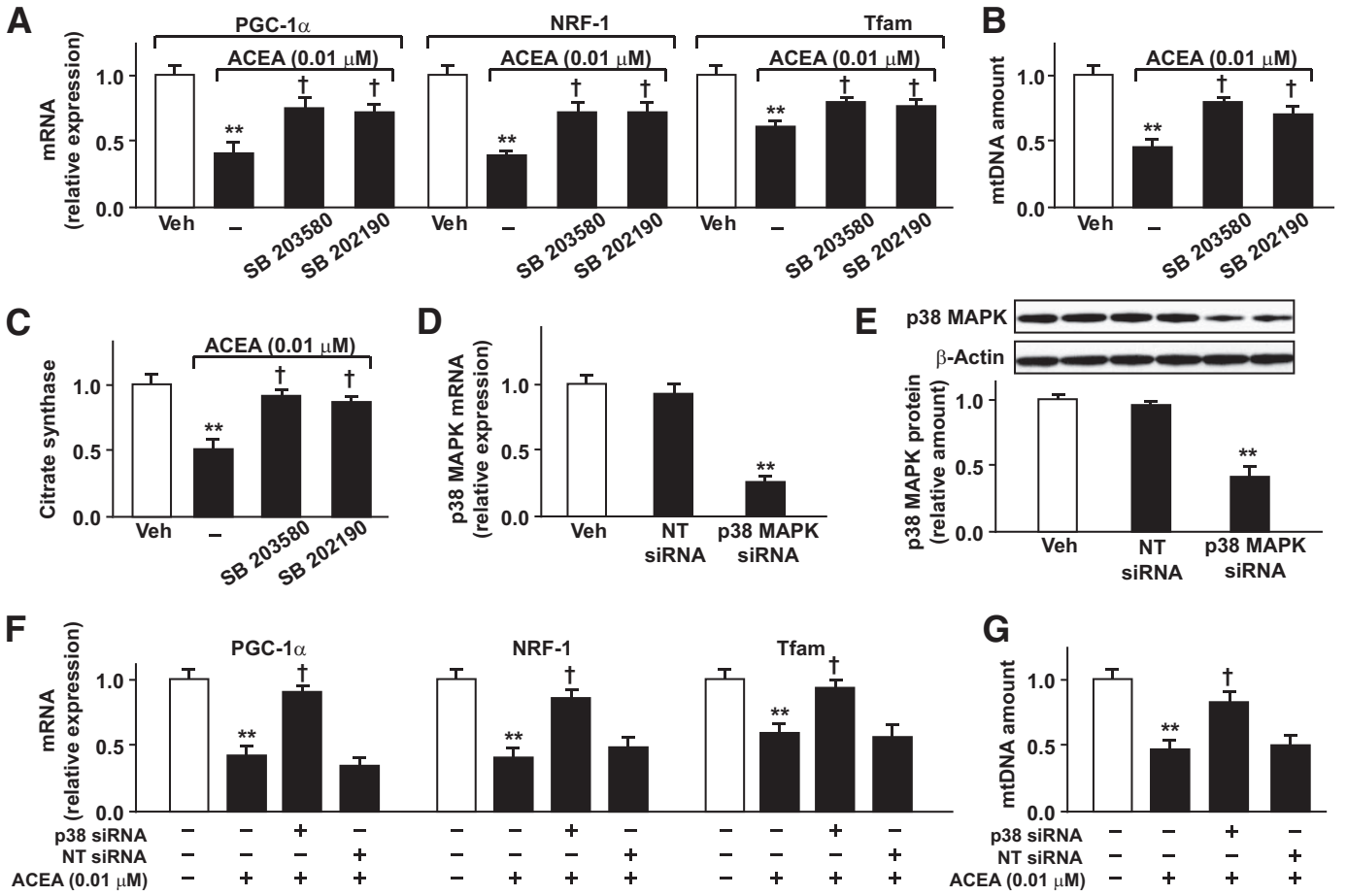

FIG. 5. Inhibition of p38 MAPK reverses the effects of ACEA on mitochondrial biogenesis in mouse white adipocytes. *A*: mRNA levels of PGC-1α, NRF-1, and Tfam. *B*: mtDNA amount. *C*: Citrate synthase in white adipocytes treated with ACEA for 16 h in the presence or absence of 10 μmol/l SB203580 or SB202190 ($n = 5$ experiments; $^{**}P < 0.01$ vs. vehicle-treated cells and $\dagger P < 0.05$ vs. ACEA-treated cells). *D* and *E*: Efficacy of p38α MAPK siRNA (NT, nontargeting siRNA). *D*: Quantitative RT-PCR ($n = 5$ experiments; $^{**}P < 0.01$ vs. vehicle. *E*: Anti–p38α MAPK immunoblots (one experiment representative of five reproducible ones, with bars showing densitometric analysis) ($^{**}P < 0.01$ vs. vehicle). *F* and *G*: Effect of p38α MAPK siRNA on ACEA-induced reductions in PGC-1α, NRF-1, Tfam mRNA expression, and mtDNA amount. $^{**}P < 0.01$ vs. vehicle-treated cells (−). $\dagger P < 0.05$ vs. ACEA-treated cells. All data represent means ± SEM.

which is less expressed in the WAT of obese humans (29) and shows reduced activity in the liver of HFD mice (30) compared with lean controls. Thus, it is possible that ACEA could undergo enhanced FAAH degradation in lean mice. Further, differences have been found in FAAH expression between visceral and subcutaneous WAT of HFD mice, possibly contributing to the observation that while the endocannabinoid system is overactive in visceral fat, it seems to be hypoactive in the subcutaneous adipose tissue (22,31). Further work will be required to clarify this complex point.

Multiple lines of evidence support the hypothesis that mitochondrial dysfunction is a key feature of obesity, insulin resistance, and type 2 diabetes (1,27) and may contribute to reduced lipid oxidation and accumulation of adipose and/or intramyocellular lipids (32). Moreover, a key role of endocannabinoids in the regulation of energy homeostasis, at both the central and peripheral levels, has been suggested (8,33). In particular, the endocannabinoids have emerged as an important link between cell energy metabolism and obesity, insulin resistance, and type 2 diabetes (34). Elevated circulating and adipose endocannabinoid levels in obese and type 2 diabetic subjects correlate with insulin resistance (35). Moreover, the infusion of cannabinoid receptor agonists in both rodents and humans induces insulin resistance in liver, muscle, and adipose tissue (36) and inhibits the respiratory enzyme activity of different rodent tissues (brain, liver, skeletal muscle, and heart) (37), with a reduction of the oxygen consumption rates (38). Here, we demonstrated that endocannabinoids and ACEA decrease several mitochondrial biogenesis markers, including PGC-1α expression, and reduce mitochondrial function in different metabolically active tissues. Our previous studies showed that PGC-1α expression was reduced in WAT from mice with either genetic or diet-induced obesity (27)—a result recently strenghtened by the observation that adipose expression of PGC-1α and mitochondrial genes is decreased in obese compared with nonobese cotwins (39).

Notably, while CB1 receptor expression increases with adipocyte differentiation (15,22), CB1 receptor stimulation increases adipogenesis (15,22). Our results with ACEA suggest that the CB1 receptor may be involved in adipose mitochondrial biogenesis downregulation. Nonetheless, a robust knockdown of the CB1 receptor did not completely reduce the inhibitory effects of ACEA on eNOS expression and mitochondrial biogenesis. Although ACEA is described as a selective CB1 receptor agonist (16), one cannot exclude that either CB2 receptor or cannabinoid receptor–independent signaling pathways may be partly

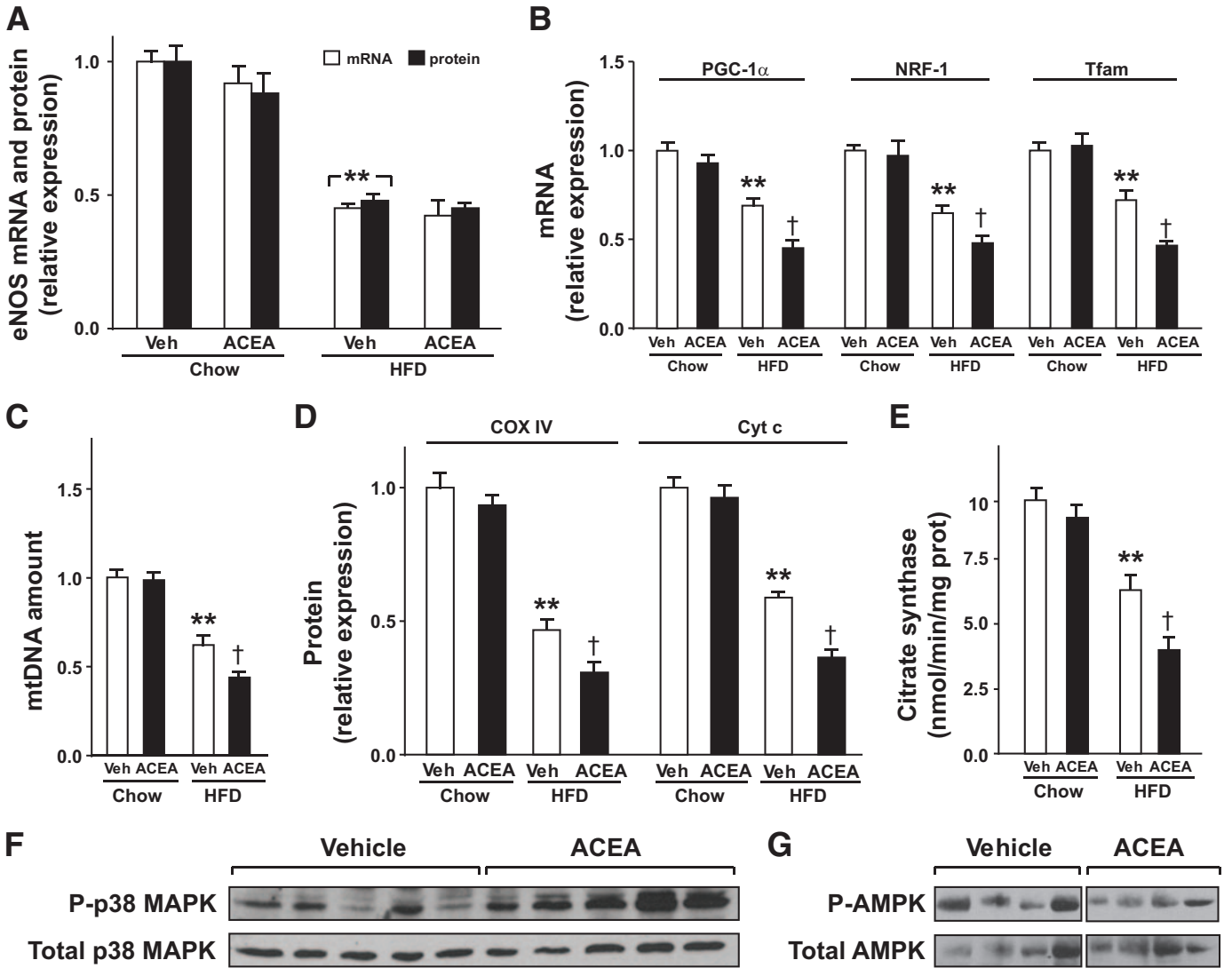

FIG. 6. CB1 receptor stimulation downregulates mitochondrial biogenesis in WAT of obese mice. *A*: eNOS mRNA, analyzed by means of quantitative RT-PCR, and eNOS protein level, detected by immunoblot with densitometric analysis, in WAT of both ACEA- and vehicle-treated mice on a chow regular diet or HFD (n = 8 animals; **P < 0.01 vs. vehicle-treated mice on a chow regular diet). *B* and *C*: PGC-1α, NRF-1, and Tfam mRNA levels and mtDNA amount in WAT of both ACEA- and vehicle-treated mice on a chow regular diet or HFD (n = 8 animals; **P < 0.01 vs. vehicle-treated mice on a chow regular diet and †P < 0.05 vs. vehicle-treated mice on a HFD). *D*: COX IV and Cyt c protein levels detected by immunoblot with densitometric analysis (n = 3 experiments; **P < 0.01 vs. vehicle-treated mice on a chow regular diet and †P < 0.05 vs. vehicle-treated mice on a HFD). *E*: Citrate synthase activity (n = 3 experiments; **P < 0.01 vs. vehicle-treated mice on a chow regular diet and †P < 0.05 vs. vehicle-treated mice on a HFD). *F*: p38 MAPK phosphorylation in WAT of vehicle- and ACEA-treated mice on a HFD. *G*: AMPK phosphorylation in WAT of vehicle- and ACEA-treated mice on a HFD. All data represent means ± SEM.

involved in the control of eNOS-mediated mitochondrial biogenesis by ACEA. CB2 receptors were downregulated by prolonged exposure to ACEA, although this may be linked to the CB1-induced adipocyte differentiation (40), which is accompanied by CB2 downregulation (22,40). Moreover, the present results argue against the involvement of TRPV1, which can be stimulated by ACEA (23) and is expressed in low amounts in adipocytes (24). The TRPV1 activation would have been able to explain the reversed concentration-response curve of ACEA. Although CB1 receptor downregulation may not be ruled out, the reason for such a behavior remains an open question. On the other hand, endocannabinoids, such as AEA and 2-AG, are produced upon demand through the hydrolysis of precursor *N*-arachidonoyl-phosphatidylethanolamine (16) and may be taken up into the cells by simple diffusion or through specific membrane transporter (41). Intriguingly, endocannabinoids and synthetic cannabinoids may bind to transcription factors (i.e., PPAR-γ) (42) or cause changes in integrated mitochondrial function, directly, in the absence of cannabinoid receptors (43).

Our present findings strongly suggest that the mitochondrial biogenesis deficit induced by ACEA is a consequence of a deficit in the NO-generating system. Not only does ACEA downregulate eNOS expression but NO donors are able to counteract the ACEA effects on mitochondrial biogenesis in white adipocytes. Previous studies have shown that NO stimulates cellular AEA uptake and degradation (44). Therefore, based on the present results, there might be a vicious circle through which ACEA, by reducing NO production, prevents its own degradation (as well as that of endogenous cannabinoids), thus possibly amplifying its own effects, especially in HFD mice, where eNOS expression is reduced.

Although NO has been shown to increase p38 MAPK activity in endothelial cells (25), other groups have re-

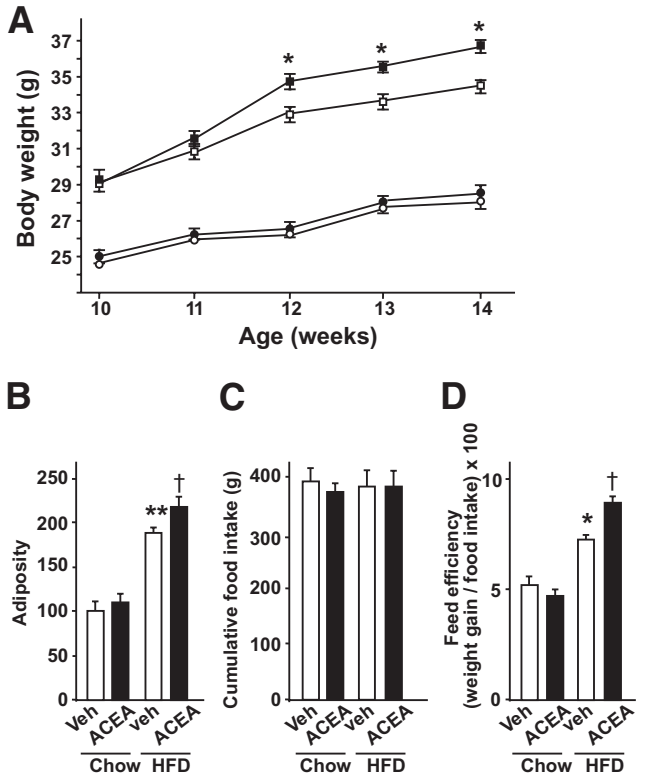

FIG. 7. CB1 receptor stimulation increases body weight in obese mice. *A*: Body weight of ACEA- or vehicle-treated mice on a HFD compared with vehicle-treated mice on a chow regular diet (n = 10 animals per group; *P < 0.05 vs. vehicle-treated mice on a HFD). ○, chow plus vehicle; ●, chow plus ACEA; □, HFD plus vehicle; ■, HFD plus ACEA. *B–D*: Adiposity (expressed as percentage of weight of visceral and subcutaneous fat when value of vehicle (Veh)-treated mice on chow regular diet is 100), cumulative food intake, and feed efficiency (n = 8 animals per group; *P < 0.05 **P < 0.01 vs. vehicle-treated mice on a chow regular diet and †P < 0.05 vs. vehicle-treated mice on a HFD).

ported that eNOS inhibition increases p38 MAPK activity in cardiomyocytes (4). We now demonstrate that sustained activation of p38 MAPK by ACEA occurs in parallel with reductions in eNOS and PGC-1α. Moreover, using *1*) two inhibitors of p38 MAPK activity, and *2*) siRNA-mediated reduction in p38α MAPK expression, we show that p38 MAPK can mediate ACEA-induced decreases in mitochondrial biogenesis parameters, including PGC-1α expression. Interestingly, our data are in line with a recent study demonstrating that activation of p38 MAPK contributed to palmitate-mediated reduction of PGC-1α in skeletal muscle cells (5). We show here that p38 MAPK phosphorylation is increased by ACEA treatment in WAT, muscle, and liver of HFD-fed mice. Moreover, p38 MAPK phosphorylation is increased in WAT and mature white adipocytes of eNOS knockout compared with wild-type mice, and ACEA is unable to further increase p38 MAPK phosphorylation in primary adipocytes obtained from $eNOS^{-/-}$ mice. This inability of ACEA was accompanied by the lack of further inhibitory effects on the already downregulated mitochondrial biogenesis in adipocytes from $eNOS^{-/-}$ mice. These findings support the notion that p38 MAPK may be a potential antiobesity target, as suggested by others (45,46). Taken together, our data demonstrate that the ACEA-mediated eNOS decrease results in sustained activation of p38 MAPK, which may serve as a negative transcriptional regulator of PGC-1α and downstream mitochondrial gene expression, in adipocytes. AMPK, another enzyme central to cellular bioenergetics (7), was reported to increase eNOS activity (6), which is consistent with the observation that CB1 blockade activates AMPK (14). We showed here that AMPK activity, measured as Thr172 phosphorylation, was reduced in the metabolically active tissues of ACEA-treated HFD mice. The clinical implications of our results would be strengthened by altering eNOS, p38 MAPK, and/or AMPK pathways in HFD mice to assess possible improvement of mitochondrial biogenesis and reduction of weight gain.

It is interesting that basal p38 MAPK phosphorylation is increased in adipocytes from type 2 diabetic subjects in association with decreased insulin receptor substrate-1 and GLUT4 content (47). In addition, high-fat feeding in rats increases p38 MAPK phosphorylation in heart (48), and p38 activation is associated with hepatic insulin resistance (49). Also, in view of the present data, the fact that a HFD enhances p38 MAPK phosphorylation in the heart might be due to endocannabinoid overactivity. In fact, heart endocannabinoid levels are elevated with two different types of HFD in mice (50). Thus, our findings support the notion that impaired mitochondrial biogenesis contributes to obesity and related metabolic disorders and might help in the design of innovative drugs to selectively counteract the cannabinoid system overactivity in peripheral tissues of obese/diabetic patients.

ACKNOWLEDGMENTS

This work was supported by grants from the Ministero della Salute (to E.N. and M.O.C.) and the Cofinanziamento 2007 Programmi di Ricerca Scientifica di Rilevante Interesse Nazionale from the Ministero dell'Istruzione, dell'Università e della Ricerca (to E.N., M.O.C., and R.V.).

No potential conflicts of interest relevant to this article were reported.

L.T. designed and performed the bulk of the experiments, analyzed all data, and wrote a first draft of the manuscript. A.V. contributed to the analysis of in vitro and in vivo data and assisted with writing. M.D. contributed to in vitro studies. A.C. contributed to in vivo studies. M.R. contributed to the in vitro studies. C.P. contributed to in vivo studies. U.P., M.O.C., and R.V. contributed to the analysis of in vivo data and revised the manuscript. E.N. developed the hypothesis, designed and analyzed all data, wrote the manuscript, and supervised the project and the peer review process.

REFERENCES

1. Patti ME, Corvera S. The role of mitochondria in the pathogenesis of type 2 diabetes. Endocr Rev 2010;31:364–395
2. Nisoli E, Clementi E, Paolucci C, Cozzi V, Tonello C, Sciorati C, Bracale R, Valerio A, Francolini M, Moncada S, Carruba MO. Mitochondrial biogenesis in mammals: the role of endogenous nitric oxide. Science 2003;299: 896–899
3. Nisoli E, Falcone S, Tonello C, Cozzi V, Palomba L, Fiorani M, Pisconti A, Brunelli S, Cardile A, Francolini M, Cantoni O, Carruba MO, Moncada S, Clementi E. Mitochondrial biogenesis by NO yields functionally active mitochondria in mammals. Proc Natl Acad Sci U S A 2004;101:16507–16512
4. Wenzel S, Rohde C, Wingerning S, Roth J, Kojda G, Schlüter KD. Lack of endothelial nitric oxide synthase-derived nitric oxide formation favors hypertrophy in adult ventricular cardiomyocytes. Hypertension 2007;49: 193–200
5. Crunkhorn S, Dearie F, Mantzoros C, Gami H, da Silva WS, Espinoza D, Faucette R, Barry K, Bianco AC, Patti ME. Peroxisome proliferator activator receptor γ coactivator-1 expression is reduced in obesity: potential pathogenic role of saturated fatty acids and p38 mitogen-activated protein kinase activation. J Biol Chem 2007;282:15439–15450

6. Morrow VA, Foufelle F, Connell JM, Petrie JR, Gould GW, Salt IP. Direct activation of AMP-activated protein kinase stimulates nitric-oxide synthesis in human aortic endothelial cells. J Biol Chem 2003;278:31629–31639
7. Cantó C, Gerhart-Hines Z, Feige JN, Lagouge M, Noriega L, Milne JC, Elliott PJ, Puigserver P, Auwerx J. AMPK regulates energy expenditure by modulating NAD+ metabolism and SIRT1 activity. Nature 2009;458:1056–1060
8. Pagotto U, Marsicano G, Cota D, Lutz B, Pasquali R. The emerging role of the endocannabinoid system in endocrine regulation and energy balance. Endocr Rev 2006;27:73–100
9. Cota D, Marsicano G, Tschoep M, Grubler Y, Flachskamm C, Schubert M, Auer D, Yassouridis A, Thone-Reineke C, Ortmann S, Tomassoni F, Cervino C, Nisoli E, Linthorst AC, Pasquali R, Lutz B, Stalla GK, Pagotto U. The endogenous cannabinoid system affects energy balance via central orexigenic drive and peripheral lipogenesis. J Clin Invest 2003;112:423–431
10. Ravinet Trillou C, Delgorge C, Menet C, Arnone M, Soubrié P. CB1 cannabinoid receptor knockout in mice leads to leanness, resistance to diet-induced obesity and enhanced leptin sensitivity. Int J Obes Relat Metab Disord 2004;28:640–648
11. Ravinet Trillou C, Arnone M, Delgorge C, Gonalons N, Keane P, Maffrand JP, Soubrié P. Anti-obesity effect of SR141716, a CB1 receptor antagonist, in diet-induced obese mice. Am J Physiol Regul Integr Comp Physiol 2003;284:R345–R353
12. Jourdan T, Djaouti L, Demizieux L, Gresti J, Vergès B, Degrace P. CB1 antagonism exerts specific molecular effects on visceral and subcutaneous fat and reverses liver steatosis in diet-induced obese mice. Diabetes 2010;59:926–934
13. Esposito I, Proto MC, Gazzerro P, Laezza C, Miele C, Alberobello AT, D'Esposito V, Beguinot F, Formisano P, Bifulco M. The cannabinoid CB1 receptor antagonist rimonabant stimulates 2-deoxyglucose uptake in skeletal muscle cells by regulating the expression of phosphatidylinositol-3-kinase. Mol Pharmacol 2008;74:1678–1686
14. Tedesco L, Valerio A, Cervino C, Cardile A, Pagano C, Vettor R, Pasquali R, Carruba MO, Marsicano G, Lutz B, Pagotto U, Nisoli E. Cannabinoid type 1 receptor blockade promotes mitochondrial biogenesis through endothelial nitric oxide synthase expression in white adipocytes. Diabetes 2008;57:2028–2036
15. Matias I, Gonthier MP, Orlando P, Martiadis V, De Petrocellis L, Cervino C, Petrosino S, Hoareau L, Festy F, Pasquali R, Roche R, Maj M, Pagotto U, Monteleone P, Di Marzo V. Regulation, function, and dysregulation of endocannabinoids in models of adipose and β-pancreatic cells and in obesity and hyperglycemia. J Clin Endocrinol Metab 2006;91:3171–3180
16. Di Marzo V. The endocannabinoid system: its general strategy of action, tools for its pharmacological manipulation and potential therapeutic exploitation. Pharmacol Res 2009;60:77–84
17. Shesely EG, Maeda N, Kim HS, Desai KM, Krege JH, Laubach VE, Sherman PA, Sessa WC, Smithies O. Elevated blood pressures in mice lacking endothelial nitric oxide synthase. Proc Natl Acad Sci U S A 1996;93:13176–13181
18. Arévalo-Martín A, Vela JM, Molina-Holgado E, Borrell J, Guaza C. Therapeutic action of cannabinoids in a murine model of multiple sclerosis. J Neurosci 2003;23:2511–2516
19. McClain DA, Hazel M, Parker G, Cooksey RC. Adipocytes with increased hexosamine flux exhibit insulin resistance, increased glucose uptake, and increased synthesis and storage of lipid. Am J Physiol Endocrinol Metab 2005;288:E973–E979
20. Scarpulla RC. Transcriptional paradigms in mammalian mitochondrial biogenesis and function. Physiol Rev 2008;88:611–638
21. Bennetzen MF, Nielsen TS, Paulsen SK, Bendix J, Fisker S, Jessen N, Lund S, Richelsen B, Pedersen SB. Reduced cannabinoid receptor 1 protein in subcutaneous adipose tissue of obese. Eur J Clin Invest 2010;40:121–126
22. Pagano C, Pilon C, Calcagno A, Urbanet R, Rossato M, Milan G, Bianchi K, Rizzuto R, Bernante P, Federspil G, Vettor R. The endogenous cannabinoid system stimulates glucose uptake in human fat cells via phosphatidylinositol 3-kinase and calcium-dependent mechanisms. J Clin Endocrinol Metab 2007;92:4810–4819
23. Price TJ, Patwardhan A, Akopian AN, Hargreaves KM, Flores CM. Modulation of trigeminal sensory neuron activity by the dual cannabinoid-vanilloid agonists anandamide, N-arachidonoyl-dopamine and arachidonyl-2-chloroethylamide. Br J Pharmacol 2004;141:1118–1130
24. Zhang LL, Yan Liu D, Ma LQ, Luo ZD, Cao TB, Zhong J, Yan ZC, Wang LJ, Zhao ZG, Zhu SJ, Schrader M, Thilo F, Zhu ZM, Tepel M. Activation of transient receptor potential vanilloid type-1 channel prevents adipogenesis and obesity. Circ Res 2007;100:1063–1070
25. Ptasinska A, Wang S, Zhang J, Wesley RA, Danner RL. Nitric oxide activation of peroxisome proliferator-activated receptor γ through a p38 MAPK signaling pathway. FASEB J 2007;21:950–961
26. Turu G, Hunyady L. Signal transduction of the CB1 cannabinoid receptor. J Mol Endocrinol 2010;44:75–85
27. Valerio A, Cardile A, Cozzi V, Bracale R, Tedesco L, Pisconti A, Palomba L, Cantoni O, Clementi E, Moncada S, Carruba MO, Nisoli E. TNF-α down-regulates eNOS expression and mitochondrial biogenesis in fat and muscle of obese rodents. J Clin Invest 2006;116:2791–2798
28. Kirkham TC, Williams CM, Fezza F, Di Marzo V. Endocannabinoid levels in rat limbic forebrain and hypothalamus in relation to fasting, feeding and satiation: stimulation of eating by 2-arachidonoyl glycerol. Br J Pharmacol 2002;136:550–557
29. Blüher M, Engeli S, Klöting N, Berndt J, Fasshauer M, Bátkai S, Pacher P, Schön MR, Jordan J, Stumvoll M. Dysregulation of the peripheral and adipose tissue endocannabinoid system in human abdominal obesity. Diabetes 2006;55:3053–3060
30. Osei-Hyiaman D, DePetrillo M, Pacher P, Liu J, Radaeva S, Bátkai S, Harvey-White J, Mackie K, Offertáler L, Wang L, Kunos G. Endocannabinoid activation at hepatic CB1 receptors stimulates fatty acid synthesis and contributes to diet-induced obesity. J Clin Invest 2005;115:1298–1305
31. Starowicz KM, Cristino L, Matias I, Capasso R, Racioppi A, Izzo AA, Di Marzo V. Endocannabinoid dysregulation in the pancreas and adipose tissue of mice fed with a high-fat diet. Obesity 2008;16:553–565
32. Jacob S, Machann J, Rett K, Brechtel K, Volk A, Renn W, Maerker E, Matthaei S, Schick F, Claussen CD, Häring HU. Association of increased intramyocellular lipid content with insulin resistance in lean nondiabetic offspring of type 2 diabetic subjects. Diabetes 1999;48:1113–1119
33. Di Marzo V, Matias I. Endocannabinoid control of food intake and energy balance. Nat Neurosci 2005;8:585–589
34. Di Marzo V. The endocannabinoid system in obesity and type 2 diabetes. Diabetologia 2008;51:1356–1367
35. Di Marzo V, Côté M, Matias I, Lemieux I, Arsenault BJ, Cartier A, Piscitelli F, Petrosino S, Alméras N, Després JP. Changes in plasma endocannabinoid levels in viscerally obese men following a 1 year lifestyle modification programme and waist circumference reduction: associations with changes in metabolic risk factors. Diabetologia 2009;52:213–217
36. Di Marzo V, Després JP. CB1 antagonists for obesity–what lessons have we learned from rimonabant? Nat Rev Endocrinol 2009;5:633–638
37. Bartova A, Birmingham MK. Effect of Δ^9-tetrahydrocannabinol on mitochondrial NADH-oxidase activity. J Biol Chem 1976;251:5002–5006
38. Chiu P, Karler R, Craven C, Olsen DM, Turkanis SA. The influence of Δ^9-tetrahydrocannabinol, cannabinol and cannabidiol on tissue oxygen consumption. Res Commun Chem Pathol Pharmacol 1975;12:267–286
39. Mustelin L, Pietiläinen KH, Rissanen A, Sovijärvi AR, Piirilä P, Naukkarinen J, Peltonen L, Kaprio J, Yki-Järvinen H. Acquired obesity and poor physical fitness impair expression of genes of mitochondrial oxidative phosphorylation in monozygotic twins discordant for obesity. Am J Physiol Endocrinol Metab 2008;295:E148–E154
40. Karaliota S, Siafaka-Kapadai A, Gontinou C, Psarra K, Mavri-Vavayanni M. Anandamide increases the differentiation of rat adipocytes and causes PPARγ and CB1 receptor upregulation. Obesity 2009;17:1830–1838
41. Hillard CJ, Jarrahian A. Cellular accumulation of anandamide: consensus and controversy. Br J Pharmacol 2003;140:802–808
42. Bouaboula M, Hilairet S, Marchand J, Fajas L, Le Fur G, Casellas P. Anandamide induced PPARγ transcriptional activation and 3T3–L1 preadipocyte differentiation. Eur J Pharmacol 2005;517:174–181
43. Athanasiou A, Clarke AB, Turner AE, Kumaran NM, Vakilpour S, Smith PA, Bagiokou D, Bradshaw TD, Westwell AD, Fang L, Lobo DN, Constantinescu CS, Calabrese V, Loesch A, Alexander SP, Clothier RH, Kendall DA, Bates TE. Cannabinoid receptor agonists are mitochondrial inhibitors: a unified hypothesis of how cannabinoids modulate mitochondrial function and induce cell death. Biochem Biophys Res Commun 2007;364:131–137
44. Maccarrone M, Bari M, Lorenzon T, Bisogno T, Di Marzo V, Finazzi-Agrò A. Anandamide uptake by human endothelial cells and its regulation by nitric oxide. J Biol Chem 2000;275:13484–13492
45. Robidoux J, Cao W, Quan H, Daniel KW, Moukdar F, Bai X, Floering LM, Collins S. Selective activation of mitogen-activated protein (MAP) kinase kinase 3 and p38α MAP kinase is essential for cyclic AMP-dependent UCP1 expression in adipocytes. Mol Cell Biol 2005;25:5466–5479
46. Maekawa T, Jin W, Ishii S. The role of ATF-2 family transcription factors in adipocyte differentiation: anti-obesity effects of p38 inhibitors. Mol Cell Biol 2010;30:613–625
47. Carlson CJ, Koterski S, Sciotti RJ, Poccard GB, Rondinone CM. Enhanced basal activation of mitogen-activated protein kinases in adipocytes from type 2 diabetes: potential role of p38 in the downregulation of GLUT4 expression. Diabetes 2003;52:634–641

48. Li SY, Liu Y, Sigmon VK, McCort A, Ren J. High-fat diet enhances visceral advanced glycation end products, nuclear O-Glc-Nac modification, p38 mitogen-activated protein kinase activation and apoptosis. Diabetes Obes Metab 2005;7:448–454
49. Liu HY, Collins QF, Xiong Y, Moukdar F, Lupo EG Jr, Liu Z, Cao W. Prolonged treatment of primary hepatocytes with oleate induces insulin resistance through p38 mitogen-activated protein kinase. J Biol Chem 2007;282:14205–14212
50. Matias I, Petrosino S, Racioppi A, Capasso R, Izzo AA, Di Marzo V. Dysregulation of peripheral endocannabinoid levels in hyperglycemia and obesity: effect of high fat diets. Mol Cell Endocrinol 2008;286:S66–S78